

Photoreactive coating for high-contrast spatial patterning of microfluidic device wettability†

Adam R. Abate,^a Amber T. Krummel,^a Daeyeon Lee,^a Manuel Marquez,^{bc} Christian Holtze^d and David A. Weitz^{*a}

Received 5th August 2008, Accepted 1st October 2008

First published as an Advance Article on the web 17th October 2008

DOI: 10.1039/b813405g

For many applications in microfluidics, the wettability of the devices must be spatially controlled. We introduce a photoreactive sol–gel coating that enables high-contrast spatial patterning of microfluidic device wettability.

Microfluidic devices can form, merge, and sort picoliter droplets with exquisite precision and at kilohertz rates. This combination of speed and control is very useful for high-throughput screening,¹ for the discovery of new drugs,² the genotyping of unknown organisms,³ and the directed evolution of enzymes and cells.⁴ A particularly convenient method for fabricating microfluidic devices is soft-lithography in poly(dimethylsiloxane) (PDMS). PDMS has several advantages as a building material for microfluidic devices. It is highly biocompatible, due to its inertness and permeability to gases.⁵ It is transparent, enabling convenient optical visualization of the processes inside the devices. With soft-lithography, sophisticated device prototypes can be fabricated quickly, easily, and at very low cost.⁵

However, for many applications, the default properties of PDMS are inappropriate, and the devices must be functionalized to control their wettability. For example, to produce inverse water-in-fluorocarbon oil emulsions, which are very useful as reactor vessels for high-throughput biology and chemistry,⁴ the devices must be functionalized to be both hydrophobic and fluorophilic.⁶ Other applications require that the device wettability be controlled spatially, to have different wettability in different regions. For example, to produce double emulsions, which consist of drops of oil and water assembled into a core–shell structure,^{6,7} the devices must be hydrophilic in some regions and hydrophobic in others.^{6,8} However, functionalization of PDMS is very difficult due to its inertness,⁹ and methods to spatially pattern the surface properties of PDMS devices yield channels with only marginal contrasts in wettability,⁶ and of limited usefulness.

In this article we introduce a method to spatially pattern high contrasts in the wettability of PDMS microfluidic devices. We coat the PDMS devices with a sol–gel layer that is functionalized with

fluorinated and photoreactive silanes. These silanes allow us to tailor the surface chemistry of the interface and to use lithographic techniques to spatially pattern the wettability. To demonstrate the utility of this approach, we fluorinate the surfaces of a microfluidic device and spatially pattern its wettability. Using this device, we produce fluorinated oil double emulsions.

The sol–gel coating consists of a dense network of functionalized silanes, and is an optimal platform for tailoring the surface chemistry of the channel interface: to tailor the coating to the particular application, we choose the appropriate functional silanes for the sol–gel. In addition, to enable the wettability of the channels to be spatially patterned, we also include photoinitiator-silanes in the sol–gel; like the other functional silanes, the photoinitiator-silanes are incorporated into the sol–gel layer as it is deposited on the microchannel walls. When exposed to UV light, the photoinitiators release radicals that, in the presence of a monomer, initiate polymerization. The polymers grow from the interface and are tethered to the sol–gel through permanent covalent bonds with the photoinitiator-silanes. The resulting interface has the chemical properties and wettability of the grafted polymers. For the photoreactive coating, we couple a photoinitiator to a silane by combining 11.0 g Irgacure 2959 photoinitiator, 0.01 g hydroquinone, and 49.4 μ L dibutyltin dilaurate in 20.0 mL of dry chloroform. The mixture is stirred under nitrogen until it is homogenous. We then slowly add 12.1 mL of 3-(triethoxysilyl)propyl isocyanate over 30 min while continuing to stir. The mixture is heated to 50 °C and stirred for an additional 3 h to allow the reaction to complete. The primary alcohol of the Irgacure reacts with the isocyanate group, forming a urethane bond¹⁰ that covalently links the photoinitiator to the silane. To concentrate the reaction product, the chloroform is removed under vacuum, yielding a yellowish solid which we use without further purification. To prepare the photoreactive sol–gel mixture, we combine 1 mL tetraethylorthosilicate (TEOS), 1 mL methyltriethoxysilane (MTES), 0.5 g photoinitiator-silane, 0.5 mL (heptadecafluoro-1,1,2,2-tetrahydrodecyl)triethoxysilane, 2 mL trifluoroethanol, 1 mL pH 2 HCl aqueous. To speed mixing, we set a hotplate to 200 °C and alternate heating and shaking the mixture until it turns clear. The PDMS channels are treated with oxygen plasma to generate silanol groups just before they are sealed by bonding to a glass slide.⁹ The bonded device is then immediately flushed with the photoreactive sol–gel mixture and allowed to sit for 2 min. The device is then placed on a hotplate set to 220 °C. The high temperature of the hotplate vaporizes the solvent in the channels and cures the coating on the walls; this produces a fluorinated interface that is, by default, very hydrophobic. To spatially pattern the wettability, we graft hydrophilic patches of polyacrylic acid (PAA) onto the hydrophobic sol–gel

^aSchool of Engineering and Applied Sciences/Department of Physics, Harvard University, Cambridge, Massachusetts, USA. E-mail: weitz@seas.harvard.edu; Fax: +1 617 4953275; Tel: +1 617 496 2842

^bNIST Center for Theoretical and Computational Nanosciences, Gaithersburg, MD, 20899, USA

^cHarrington Department of Bioengineering, Arizona State University and Center for Integrated Nanotechnologies, Los Alamos National Laboratory, Los Alamos, NM, 87545, USA

^dBASF, Ludwigshafen, Germany

† Electronic supplementary information (ESI) available: Movies available as supplementary information are Polymerization.avi and Double emulsions 2 to 6.avi. See DOI: 10.1039/b813405g

interface. To graft the hydrophilic polymers, we fill the devices with acrylic acid monomer solution consisting of 0.2 mL of acrylic acid with 0.8 mL 5 mM NaIO₄ H₂O, 1 mL ethanol, 0.5 mL acetone and 0.05 g benzophenone. We then expose the channels UV light (see ESI, polymerization.avi†) wherever we desire the wettability to be hydrophilic.^{11,12}

The thickness and uniformity of the coating deposited on the channel interface depend on the viscosity of the sol-gel liquid and how the coating is deposited.⁹ To study the coating as it is deposited on the channel walls, we image channel cross-sections using scanning electron microscopy (SEM). The uncoated PDMS channel has a rectangular cross-section, due to its stamped fabrication, as shown in Fig. 1a. The wavy pattern on the side walls is an artifact of the soft-lithography process, and can be clearly seen in the magnified view of Fig. 1b. By contrast, for the coated and PAA grafted channel the rectangular corners are rounded and the wavy pattern is smoothed over; this occurs because the coating liquid wets the surface and collects in regions of high curvature, as shown in Fig. 1c and in the magnified view of Fig. 1d.⁹

The coating and spatial patterning of the interface significantly modifies its wettability, as confirmed by contact-angle measurement performed with water droplets in air. The incorporation of fluorosilanes into the sol-gel produces a coating that is hydrophobic and fluorophilic by default; thus, the water drop beads up¹³ forming a contact angle of $105 \pm 1^\circ$, as shown in Fig. 2a. By contrast, after graft polymerization of PAA, the coating surface is hydrophilic, so that the water drop spreads out,¹⁴ forming a hydrophilic contact angle of $22 \pm 5^\circ$, as shown in Fig. 2b. Polymerization thus changes the contact angle by 83° ; this is much larger than can be achieved by grafting polymers to the PDMS network directly,⁶ and is sufficient for the emulsification of fluorocarbon, hydrocarbon, and silicon oils.

The properties of the sol-gel interface depend on its topographical structure. The topography of a sol-gel coating can be tuned over a large range by tuning its chemistry and cure temperature. This enables the interface to be tailored to have open or closed pores, from the angstrom to the micron scales.^{15–17} To produce a coating that is smooth and homogenous, we choose an acidic catalyst and a moderate cure temperature. We investigate the topographical

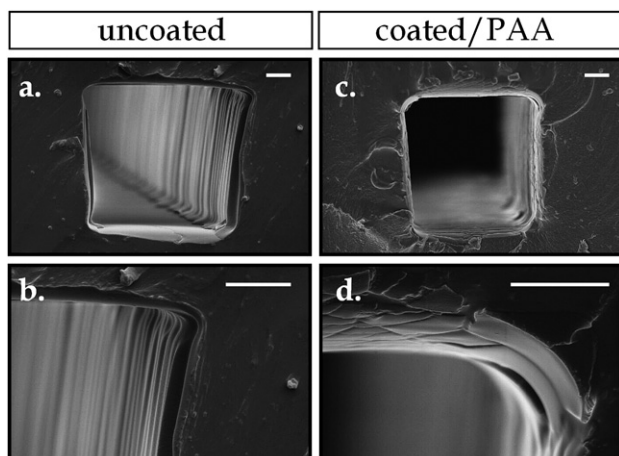


Fig. 1 SEM images of channel cross sections; scale bars denote 5 μm . (a) Uncoated PDMS channel cross-section and (b) magnified view of upper right corner. (c) Coated, PAA functionalized PDMS channel and (d) magnified view of upper right corner; the corner is rounded because the sol-gel wets the surface and collects in regions of high curvature.

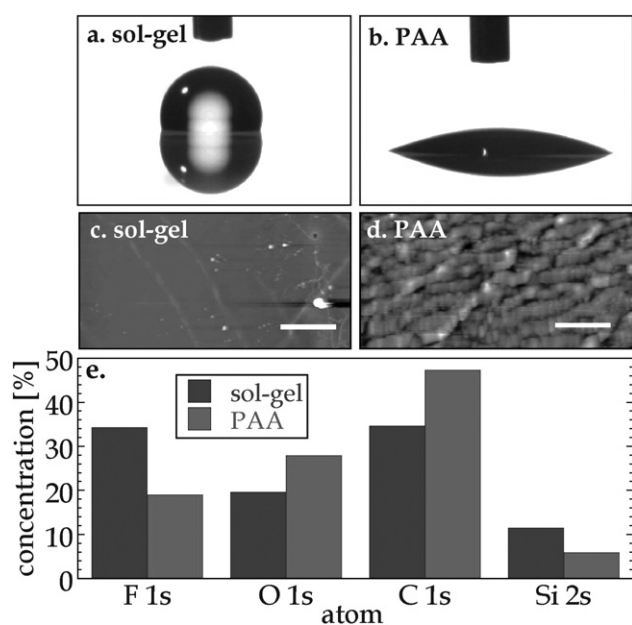


Fig. 2 Contact angle measurement of water droplets in air on (a) sol-gel coated substrate with contact angle 105° and (b) PAA grafted substrate with contact angle 22° . AFM images of (c) sol-gel coated and (d) PAA grafted microchannels. The images show a $10 \times 20 \mu\text{m}$ area at high resolution; the dark to light color scale maps to feature heights of -150 to 150 nm . (e) Surface concentrations of atoms on sol-gel coated and PAA functionalized substrates, measured with XPS; fluorine (F 1s), oxygen (O 1s), carbon (C 1s), and silicon (Si 2s).

structure of the coating as deposited in a microchannel by imaging the channel interface with atomic force microscopy (AFM). The sol-gel surface is smooth and homogenous, as shown in the AFM image of the sol-gel coated channel in Fig. 2c. By contrast, after polymerization, the interface has a complex three-dimensional structure, with large polymer aggregates on the hundred nanometer scale, as shown in the AFM image of the PAA grafted interface in Fig. 2d. Graft-polymerization onto the sol-gel thus significantly modifies its topographical structure.

Graft-polymerization onto the sol-gel also significantly modifies its interfacial chemistry. To investigate this, we use X-ray photoelectron spectroscopy (XPS). The X-ray beam penetrates the upper-most layer of the substrate and provides a detailed and accurate measure of the concentration of atoms present on the interface.¹⁸ The native sol-gel coating shows a pronounced concentration of fluorine and a small concentration of silica, suggesting the low surface energy fluorocarbons orient outwards during gelation, forming a fluorinated surface that masks the siloxane backbone of the sol-gel, as shown in Fig. 2e. By contrast, the polymerized region shows a reduction in fluorine and increase in carbon, indicating hydrophilic PAA on the interface, as shown in Fig. 2e. The carbon peak also shifts to higher photoelectron energy, as expected from the high energy carbonyl bonds that make up the PAA.^{14,19} Thus, surface initiated polymerization significantly alters the chemistry, topography, and wettability of the channel interface.

An important and valuable feature of this method is the ability to spatially control polymerization, thereby enabling spatial patterning of the device wettability. To achieve this spatial control, we project spatially patterned UV light onto the device. As a demonstration, we

spatially pattern a long, straight microfluidic channel with several patches of PAA. We flush the patterned channel with toluidine blue, a dye that electrostatically binds to PAA.²⁰ Because the PAA exists only in the patterned patches of the channel, only these patches of the channel stain. We show a magnified view of the border of a polymerized patch in Fig. 3a. To quantify the spatial resolution of the grafting, we compute the average intensity across the channel and plot as a function of location down the channel, given in Fig. 3b. From the plot and the image, we estimate the resolution of the graft-polymerization to be 5 μm . With more precise optics, the resolution can be improved to smaller than a micron.

The sol-gel coating enables us to independently control the channel surface chemistry and to spatially pattern device wettability. As a demonstration of the utility of this approach for functionalizing

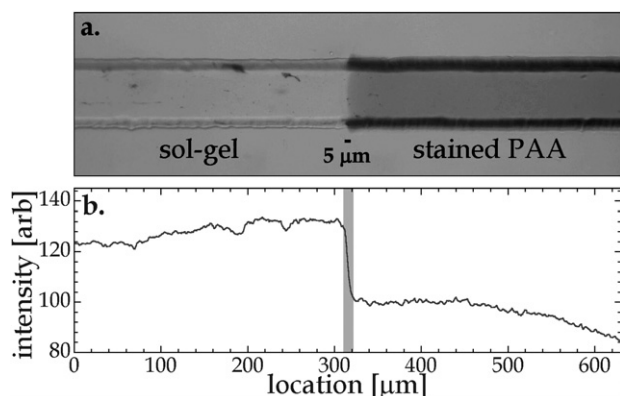


Fig. 3 (a) Photomicrograph of a sol-gel coated channel. PAA has been grafted to the right half of the channel using UV-initiated graft polymerization. The grafted polymer is dyed with toluidine blue, a dye that preferentially stains PAA. (b) Average grayscale intensity across the channel as a function of location along the channel.

microfluidic channels, we construct a microfluidic device to produce double emulsions using fluorinated oil. Fluorinated oil and water emulsions are very useful for microfluidic applications in biology, due to their stability, inertness, and permeability to gases.²¹ However, their formation requires the interface to be both hydrophobic and fluorophilic.^{6,8} To produce double emulsions, it is also essential to spatially pattern the wettability of the device. For the emulsions, we use water and fluorocarbon oil (Fluorinert FC40) stabilized by surfactants Zonyl FSN-100 (Sigma-Aldrich) and Krytox 157FSL (Dupont), respectively. We construct a double emulsion device consisting of two flow-focus drop makers arranged in series. We graft PAA onto the first drop formation stage, making it hydrophilic; the default properties of the sol-gel make the second stage both hydrophobic and fluorophilic; the device structure is illustrated in Fig. 4a. The first drop maker produces a direct fluorocarbon oil-in-water emulsion, as shown in Fig. 4b and in the magnified view of Fig. 4c. By contrast, the hydrophobic second drop maker emulsifies the water continuous phase from the first drop maker, encapsulating the oil drops, and forming monodisperse O/W/O double emulsions, as shown in Fig. 4b-d. We can also form W/O/W emulsions by grafting PAA onto only the second drop maker.^{6,8} The double emulsion formation is stable, as shown in the movie available as ESI.† The double emulsion drops produced are also highly monodisperse, as demonstrated by their hexagonal ordering in Fig. 4d.

The photoreactive sol-gel coating enables tailoring of the surface chemistry and spatial patterning of the wettability of PDMS microfluidic devices. This allows channels to have distinct functional properties in different regions; this is useful for the fabrication of sensing devices,²² the separation of analytes,²³ and as we have shown here, the formation of double emulsions. Moreover, the stamped fabrication, sol-gel coating, and lithographic patterning are all scalable to massively parallelized microfluidic devices. Such devices should enable the industrialization of microfluidic products, such as double emulsion templated core-shell structures.⁷ These are useful for

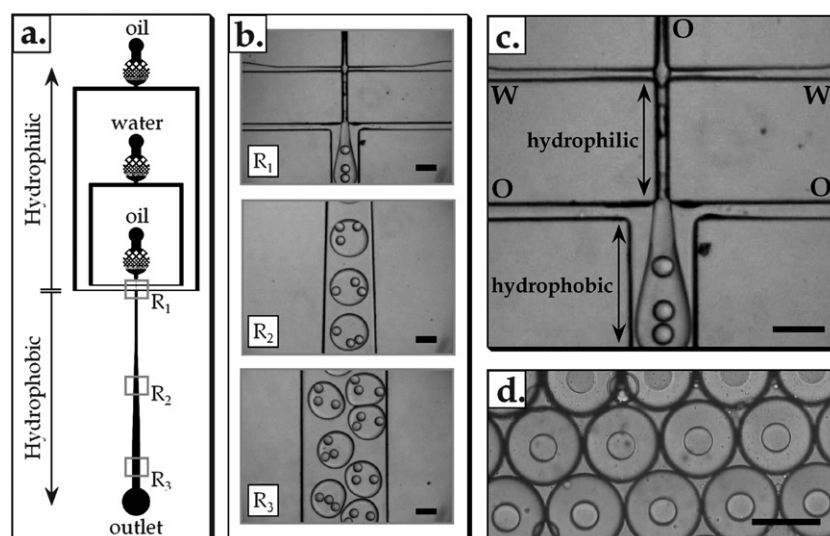


Fig. 4 (a) Diagram of sol-gel coated device. The upper half of the device is hydrophilic due to graft-polymerization of PAA. The bottom half of the device is hydrophobic due to the default properties of the sol-gel coating. (b) Photomicrograph of double emulsions being formed (R1) and flowing out of the microfluidic device (R2 and R3). (c) Magnified view of the double emulsion flow-focusing junction in R1. (d) Photomicrograph of O/W/O double emulsions; the drops crystallize due to their high monodispersity. The scale bars for all figures denote 100 μm .

the encapsulation and triggered release of precious materials, such as cosmetics, nutrients, and drugs.

Acknowledgements

This work was supported by a Human Frontiers Grant (RGP0004/2005-C102), the NSF (DMR-0602684) and (DBI-0649865), the Harvard MRSEC (DMR-0213805), and the Deutsche Forschungsgemeinschaft (DFG).

Notes and references

- 1 H. Fenniri and R. Alvarez-Puebla, *Nat. Chem. Biol.*, 2007, **3**, 247–249.
- 2 L. Mere, T. Bennett, P. Coassin, P. England, B. Hamman, T. Rink, S. Zimmerman and P. Negulescu, *Drug Discov. Today*, 1999, **4**, 363–369.
- 3 N. Y. Zhang, H. D. Tan and E. S. Yeung, *Anal. Chem.*, 1999, **71**, 1138–1145.
- 4 M. Eisenstein, *Nat. Methods*, 2006, **3**, 71–71.
- 5 D. C. Duffy, J. C. McDonald, O. J. A. Schueller and G. M. Whitesides, *Anal. Chem.*, 1998, **70**, 4974–4984.
- 6 M. Seo, C. Paquet, Z. H. Nie, S. Q. Xu and E. Kumacheva, *Soft Matter*, 2007, **3**, 986–992.
- 7 A. S. Utada, E. Lorenceau, D. R. Link, P. D. Kaplan, H. A. Stone and D. A. Weitz, *Science*, 2005, **308**, 537–541.
- 8 T. Nisisako, S. Okushima and T. Torii, *Soft Matter*, 2005, **1**, 23–27.
- 9 A. R. Abate, D. Lee, T. Do, C. Holtze and D. A. Weitz, *Lab Chip*, 2008, **8**, 516–518.
- 10 M. V. Kahraman, N. Kayaman-Apohan, Z. S. Akdemir, Y. Boztoprak and A. Gungor, *Macromol. Chem. Phys.*, 2007, **208**, 1572–1581.
- 11 G. A. Diaz-Quijada and D. D. M. Wayner, *Langmuir*, 2004, **20**, 9607–9611.
- 12 Y. L. Wang, H. H. Lai, M. Bachman, C. E. Sims, G. P. Li and N. L. Allbritton, *Anal. Chem.*, 2005, **77**, 7539–7546.
- 13 D. Anton, *Adv. Mater.*, 1998, **10**, 1197, –+.
- 14 L. J. Ward, W. C. E. Schofield, J. P. S. Badyal, A. J. Goodwin and P. J. Merlin, *Chem. Mater.*, 2003, **15**, 1466–1469.
- 15 C. J. Brinker and G. W. Scherer, *Sol-gel science: the physics and chemistry of sol-gel processing*, Academic Press, Boston, 1990, pp. xiv, 908.
- 16 J. Estella, J. C. Echeverria, M. Laguna and J. J. Garrido, *J. Non-Cryst. Solids*, 2007, **353**, 286–294.
- 17 S. Z. Yu, T. K. S. Wong, X. Hu and K. Pita, *J. Electrochem. Soc.*, 2003, **150**, F116–F121.
- 18 D. A. Skoog, F. J. Holler and T. A. Nieman, *Principles of Instrumental Analysis*, Saunders College Publishing, Philadelphia, 1997.
- 19 E. Selli, G. Mazzone, C. Oliva, F. Martini, C. Riccardi, R. Barni, B. Marcandalli and M. R. Massafra, *J. Mater. Chem.*, 2001, **11**, 1985–1991.
- 20 D. Yoo, S. S. Shiratori and M. F. Rubner, *Macromolecules*, 1998, **31**, 4309–4318.
- 21 J. G. Riess and M. P. Krafft, *Artif. Cells, Blood Substitutes, Immobilization Biotechnol.*, 1997, **25**, 43–52.
- 22 T. H. Park and M. L. Shuler, *Biotechnol. Prog.*, 2003, **19**, 243–253.
- 23 J. Rossier, F. Reymond and P. E. Michel, *Electrophoresis*, 2002, **23**, 858–867.